Feed Array Breadboard for Future Passive Microwave Radiometer Antennas

C. Cappellin[1], J. R. de Lasson [1], O. Iupikov[2], M. Ivashina[2], N. Skou[3], K. Pontoppidan[1], B. Fiorelli[4]
[1]TICRA, Copenhagen, Denmark, Email: cc@ticra.com, jrdl@ticra.com, kp@ticra.com
[2]Chalmers University of Technology, Gothenburg, Sweden, Email: oleg.iupikov@chalmers.se, marianna.ivashina@chalmers.se
[3]DTU Space, Technical University of Denmark, Lyngby, Denmark, Email: ns@space.dtu.dk
[4]ESA/ESTEC, Noordwijk, The Netherlands, Email: benedetta.fiorelli@esa.int

***Abstract*—The pattern of a 265 mm x 200 mm breadboard made of 35 x-polarized and 32 y-polarized Vivaldi antennas located above a finite ground plane is computed and measured at 6.9 GHz. The breadboard constitutes the feed array illuminating a 5 m conical scan antenna working at 6.9 GHz for next generation microwave radiometers for ocean observation. The analysis is done including mutual coupling between the elements, and in two commercial software, the MoM add-on to GRASP and CST. The breadboard is measured at the Spherical Near-Field Antenna Test Facility at the Technical University of Denmark.**

***Index Terms*—RF modelling, measurement, array.**

I. Introduction

Next generation microwave radiometers for ocean observation will need to deliver high spatial and radiometric resolution (ΔT), Sea Surface Temperature (SST) and vector wind fields, with the highest possible absolute accuracy and closer to coasts and sea ice than seen hitherto, see the requirements of TABLE I, as reported also in [1].

TABLE I. Radiometric requirements for next generation SST and wind fields observations.

Frequencies [GHz]	Pol	ΔT [K]	Accuracy [K]	3-dB Footprint [km]	Distance to coast/ice [km]
C band: 6.9 ± 0.1 7.3 ± 0.1	V and H	0.3	0.25	20	20

Current spaceborne microwave radiometers for SST and wind fields operating in C band, like AMSR-2 and WindSat for example [2][3], provide a spatial resolution, defined as the 3-dB footprint, of around 55 km, whereas less than 20 km is desirable. The radiometric resolution in C band for WindSat is around 0.7 K, while 0.3 K is needed. Moreover, current systems provide measurements not closer than around 100 km from the shore-line, because of the signal contamination provided by the antenna sidelobes illuminating the land, which is significantly warmer than the sea. There is a strong desire to reduce this distance to 20 km or less.

The spatial resolution of TABLE I can be achieved by correctly sizing the reflector antenna aperture (to 5 m), while the required radiometric resolution can be achieved by considering several simultaneous beams in the along- and across-track, either in a push-broom system, or in a multi-beam scanning system. The accuracy and distance to coast requirements can only be met by considering antenna beams with very low cross-polar component and extremely low sidelobes, which are not achievable in a traditional single feed per beam configuration [4].

In the ESA contract 4000107369-12-NL-MH run between 2013-2015 it was shown that both types of antenna systems could meet the challenging requirements of TABLE I provided the reflector antennas were illuminated by a feed array of closely spaced elements, properly excited and controlled by a digital beamformer, see [1] and [5], in a multi-feed per beam configuration. More elements take part in the formation of each beam and the same element takes part in the formation of multiple beams. The chosen array element was a half-wave dipole above an infinite ground plane, and mutual coupling between the elements was disregarded, implying identical element patterns.

The ESA activity "Focal Plane Array Bread-Board for Advanced Multiple Beam Radiometer Antenna", contracted to TICRA with Chalmers University and DTU Space (ESA contract 4000117841/16/NL/FF/gp) and just completed, has the purpose to prove the feed array concept, and verify if the radiometric requirements of TABLE I can still be met with a realistic array with non-identical element patterns.

To do this, a breadboard of the feed array was designed, analyzed, manufactured and tested, in order to validate the accuracy of the computed element patterns. It is underlined that the detailed and accurate RF modelling of the full antenna system is indeed of paramount importance for the accurate calibration of the radiometer and represents the main goal of the study. In the last part of the activity, the computed element patterns are used to find the new excitation of the array elements, and the updated radiometric performances are calculated [10]. This paper describes the work done up to the breadboard RF test. In particular, Section II focuses on the design and analysis of the radiating element chosen for the breadboard, while Section III shows the RF models of the breadboard developed with two

commercial software, the MoM add-on to GRASP and CST. In Section IV, we show the breadboard manufactured at Chalmers University, and describe the RF test that took place at the DTU-ESA Spherical Near-Field Facility at the Technical University of Denmark. Finally, in Section V we compare the element patterns of a few selected elements, as computed by GRASP and CST, with each other and with the measured data. Conclusions are drawn in Section VI.

II. Radiating Element Requirements and Design

The breadboard represents the feed array necessary to produce the beams of a 5 m conical scan antenna at 6.9 GHz. The breadboard is also representative for the feed array requested at higher frequencies for the same antenna, or for the push-broom configuration.

A list of the electrical and mechanical requirements was set up in order to study possible candidates for the array element type to be used in the breadboard, as shown in TABLE II. It is noted that the element design is optimized to minimize the cross-polarization level of the full array, while the cross-polarization level for the single element is not considered a design driver. Finally, it is observed that there is no direct requirement for the peak directivity, though it is clear that, due to an element size smaller than a wavelength, the peak directivity will not be higher than approximately 7-8 dBi.

TABLE II. Radiating Element Requirements.

Frequency	C band: 6.9 ± 0.1 & 7.3 ± 0.1 GHz
Polarization	Dual linear
Matching conditions	Amplitude of the active reflection coefficient < -10 dB for a 50 Ohm input impedance
Element size	Smaller than 0.75λ in both width and height
Feeding	Coaxial feeding
Cost	Materials, assembly and manufacturing within the budget of the project

Three antenna elements were considered as potential candidates for the breadboard, namely a crossed dipole, a patch excited cup from RUAG [6] and a Vivaldi antenna [7], see Fig. 1. These were chosen since they satisfied the requirements and their RF modelling was well-known. In spite of its single polarization and a TRL lower than the one of the patch from RUAG, the Vivaldi element was chosen for the breadboard. This was due to two important reasons: the overall cost constraints and a challenging RF modelling, which includes a shaped antenna element, a PCB with microstrip and a coaxial feeding.

Fig. 1. Candidates for the radiating element of the breadboard.

The Vivaldi element was further designed by Chalmers University, taking as outset the EMBRACE antenna element (500-1500 MHz) presented in [8], and scaling it up in frequency. The scaled element geometry was re-optimized in profile and cavity size in order to achieve low active reflection coefficient. Later on, the microstrip feeding was optimized in width, stub radius and dielectric thickness, to lower the return loss. The final design is shown in Fig. 2.

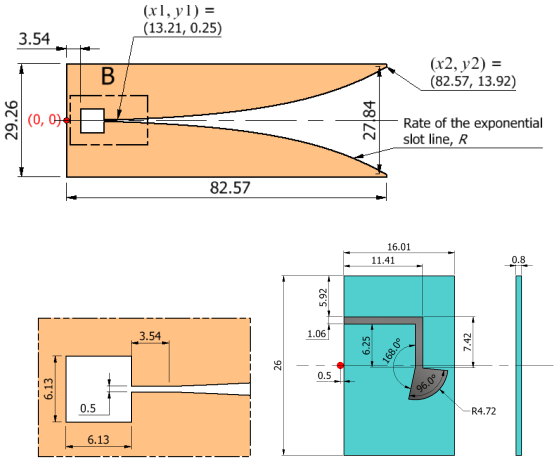

Fig. 2. Detailed geometry of the Vivaldi element: the antenna is made of aluminum with 0.4 mm thickness. The dielectric material for the PCB is Rogers RO4003 with permittivity equal to 3.55 and loss tangent equal to 0.0027. All dimensions are in millimeters (mm).

The Vivaldi element of Fig. 2 was modelled by Chalmers University in CST and analyzed above a finite size ground plane of 58 mm X 58 mm. The computed pattern at 6.9 GHz can be seen in Fig. 3, with solid (dashed) curves being the co-polar (cross-polar) component and different colors corresponding to different φ cuts.

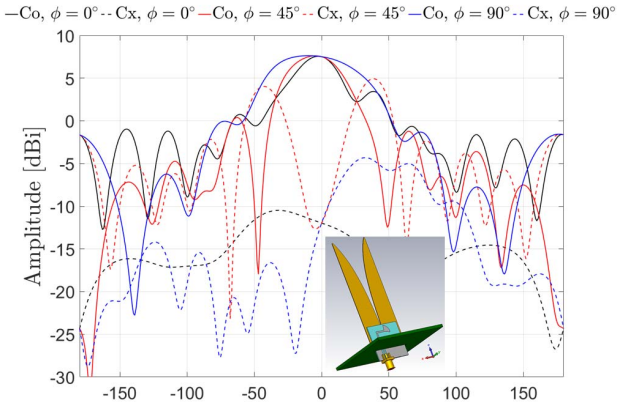

Fig. 3. Co-polar and cross-polar components of the far-field pattern of the single element computed with CST at 6.9 GHz.

We note a slight asymmetry in the patterns around θ = 0°, which we attribute to the slight feeding-induced asymmetry of the element: the dielectric slab is on one side of the blades (y-asymmetry), and the coax and microstrip are slightly displaced from the center (x-asymmetry). The co- and cross-polar component patterns vary with varying φ.

III. BREADBOARD RF MODELS

The breadboard consists of 35 x-polarized and 32 y-polarized Vivaldi antennas placed 0.67 wavelength (29.26 mm at 6.9 GHz) from each other and located on an xy-grid above a ground plane of 265 mm x 200 mm x 5 mm. Each Vivaldi element has a thickness of 0.4 mm and is excited by a coaxial waveguide with 50 Ohm characteristic impedance. This leads to 35+32= 67 SMA female connectors on the rear side of the ground plane. In addition, 26 half Vivaldi antenna elements are located at the edge of the breadboard, in direct connection to the above elements. These are dummy elements and not directly excited, and have the purpose to both reduce the edge truncation effect and to make the breadboard mechanically stiffer. The MoM add-on to GRASP and CST are used to analyze the array elements radiation patterns.

The breadboard model set up by TICRA in the MoM add-on to GRASP is seen in Fig. 4 and Fig. 5. The CST model developed by Chalmers is seen in Fig. 6. In both models, the same coaxial-microstrip connection is considered, the thickness of the Vivaldi elements and of the ground plane is included, while screws in the PCB slab are disregarded.

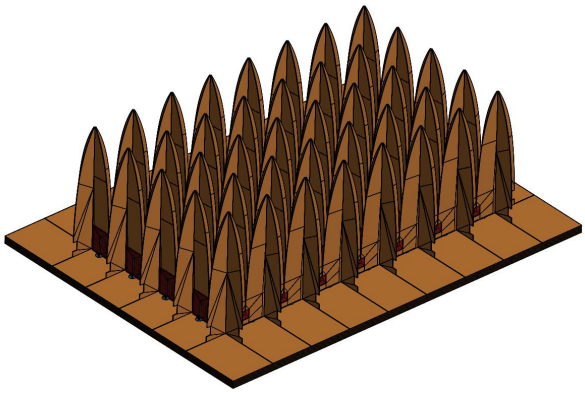

Fig. 4. Model of the breadboard in the MoM add-on to GRASP.

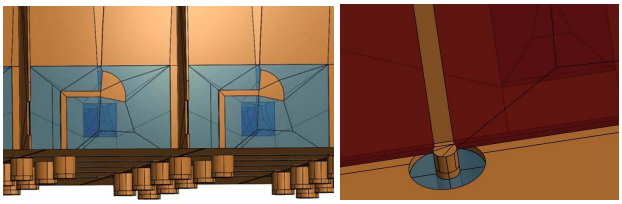

Fig. 5. Model of the breadboard in the MoM add-on to GRASP: zoom in on the microstrip and coaxial feeding.

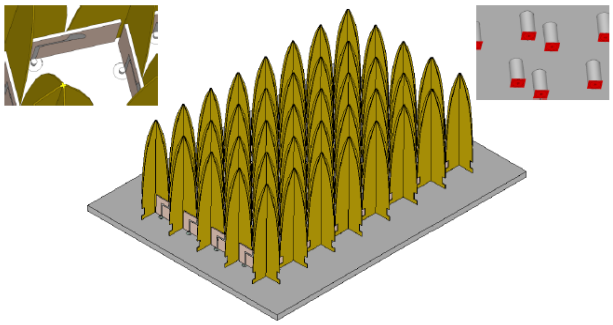

Fig. 6. Model of the breadboard in CST. All Vivaldi elements and the finite-size ground plane are visible, as well as details of the coaxial feeding.

IV. MANUFACTURING OF THE BREADBOARD AND RF TEST

The breadboard was manufactured by Chalmers University, see Fig. 7, and shipped to Denmark, to be measured in September 2017 at the DTU-ESA Spherical Near-Field Antenna Test Facility at the Technical University of Denmark [9]. The breadboard mounted on the measurement tower can be seen in Fig. 8; 14 array elements were measured in transmission mode in amplitude and phase at 6.9 GHz on a full sphere of 6 m radius.

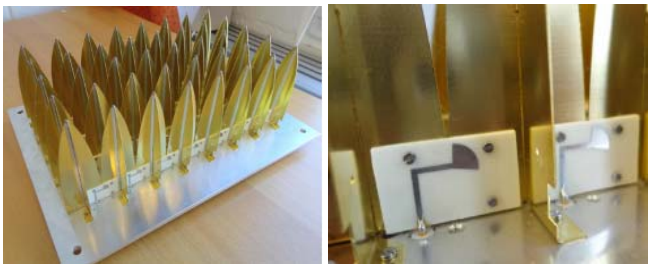

Fig. 7. Breadboard manufactured at Chalmers University, details of the feeding on the right.

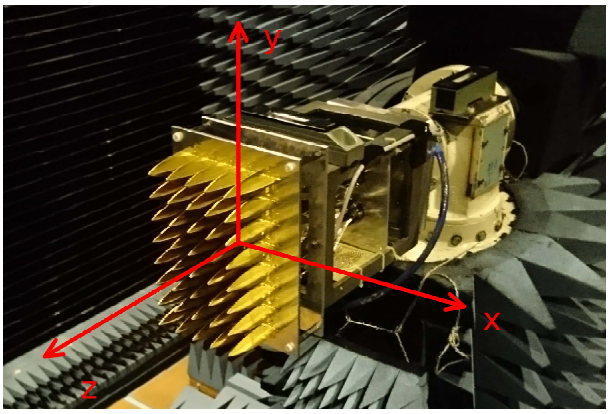

Fig. 8. Breadboard mounted on the antenna tower at the DTU-ESA Spherical Near-Field Antenna Test Facility, with the measurement coordinate system highlighted.

One element was excited and measured at a time, while all the others were matched. The elements to be measured were activated by an electromechanical switch designed by DTU Space, that is visible behind the ground plane of the

breadboard in Fig. 8: this allowed to excite the 14 elements remotely without moving the connector during the measurements.

V. Pattern Comparison

In the following, we compare the patterns of two representative array elements, as computed by GRASP and CST, with the measurements. We choose element 18, located at the center of the array, and element 35, located at the upper right corner, see Fig. 9. The patterns refer to a coordinate system with origin at the center of the ground plane, with the x-axis (y-axis) parallel to the long (short) side of the breadboard, see Fig. 9, and are expressed in Ludwig 3rd polarization.

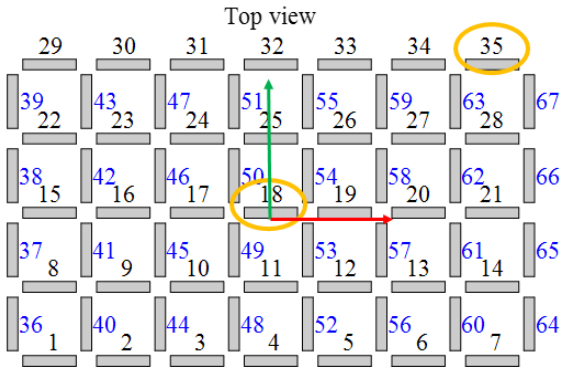

Fig. 9. Array element indexing: x-oriented Vivaldi elements are written in black and y-oriented in blue. The two elements used for pattern comparison are highlighted in yellow. The x- (red) and y-axis (green) and the origin of the reference coordinate system are shown as well.

A. Element 18

Element 18 is an x-oriented element located at the center of the array. Its amplitude pattern in dBi in the φ = 90° cut is shown in Fig. 10, with measured (GRASP) [CST] patterns shown in black (blue) [red]. It is seen that the GRASP and CST co-polar components coincide with the measured field in the [-80°:80°] range. The agreement between GRASP and CST remains excellent in the back hemisphere for negative θ values where the measured field differs slightly, while small differences between the three curves are seen in the back hemisphere for positive θ values. The cross-polar component remains at a level of -30 dB from the peak, and shows fine agreement among the three sets of curves. Similar observations were drawn for the elements close to the center of the array. The disagreement of the computed patterns with the measured pattern in part of the back hemisphere are mainly due to the presence of the measurement tower and the antenna under test support frame, which are not included in the RF models.

The currents induced on the array when the element 18 is excited (with all other elements matched) are seen in Fig. 11 in a 50 dB dynamic color range, as computed by GRASP. It is evident that the coupling with the neighboring elements is strong, affecting the pattern. This is clearly visible when comparing the pattern of Fig. 10 with the one in Fig. 3 (single element).

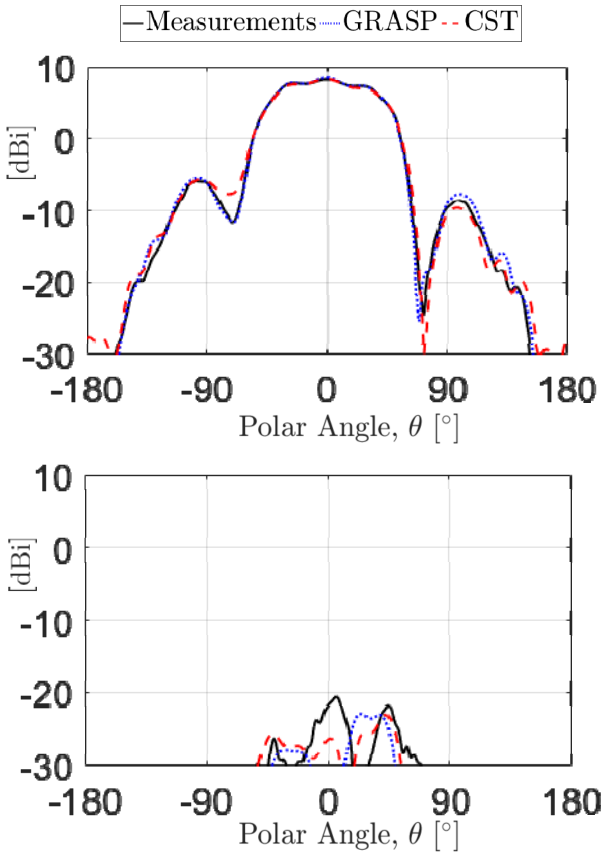

Fig. 10. Amplitude pattern in dBi in the φ = 90° cut for the center element 18 at 6.9 GHz: measured (GRASP) [CST] patterns shown in black (blue) [red]. The co-polar (cross-polar) component is shown in the top (bottom) panel.

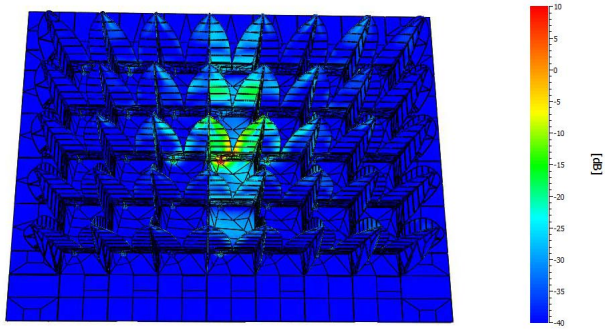

Fig. 11. Amplitude of total currents induced on the aray when element 18 is excited and the other elements are matched, computed by GRASP. The dynamic range of the color scale is 50 dB.

B. Element 35

Element 35 is an x-oriented corner element. On symmetry grounds, it performs like elements 1, 7 and 29. Its amplitude pattern in dBi in the φ = 90° cut is shown in Fig. 12, with measured (GRASP) [CST] patterns shown in black (blue) [red]. It is seen that the agreement in the co-polar pattern is excellent between the three curves for θ in the

[-80°:80°] angular region. It is again noted that GRASP and CST curves are in excellent agreement and coincide with each other in the full sphere, while the measured field differs slightly in the back hemisphere, due to the presence of the antenna under test support frame and measurement tower, which are not included in the RF models. The cross-polar component shows good agreement in ripples and peak values between all curves in the full angular domain. Similar observations can be made for the other corner elements that were measured.

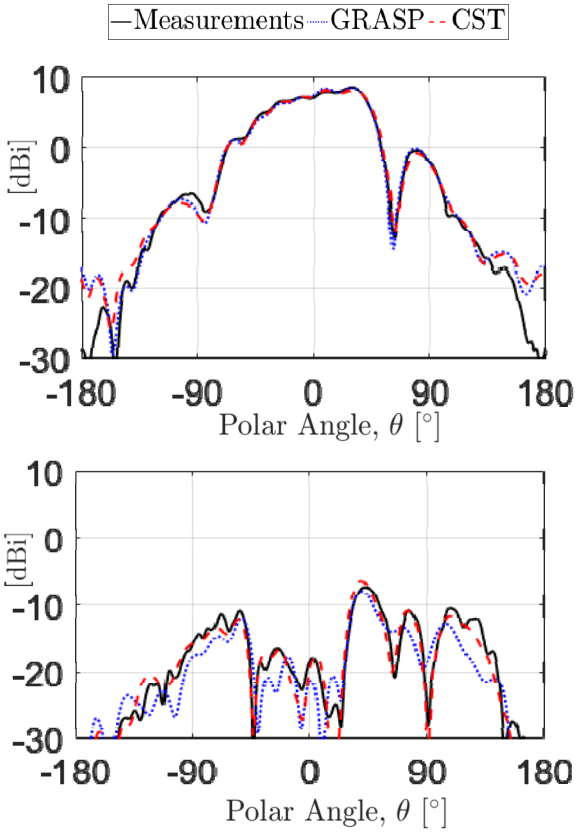

Fig. 12. Amplitude pattern in dBi in the φ = 90° cut for the corner element 35 at 6.9 GHz: measured (GRASP) [CST] patterns shown in black (blue) [red]. The co-polar (cross-polar) component is shown in the top (bottom) panel.

VI. Conclusions

The detailed design, RF analysis, manufacturing and testing of a 265 mm x 200 mm breadboard made by 35 x-polarized and 32 y-polarized Vivaldi elements located above a finite ground plane were described. The breadboard constitutes the feed array illuminating a 5 m conical scan radiometer in a multi-feed per beam configuration, for future high performance radiometric systems. The analysis of the breadboard was done at 6.9 GHz including mutual coupling between the elements and in two commercial software, the MoM add-on to GRASP and CST. The results showed that the two commercial codes provide coinciding patterns in excellent agreement with the measured field in the co-polar and cross-polar components. This was true for both corner and center elements. Small differences were observed between the computed patterns and the measured pattern in part of the back hemisphere, due to the presence of the antenna under test support frame and the measurement tower, which were not included in the computational models.

Acknowledgments

We would like to thank RUAG Space, Sweden, for providing us with the data for the patch-excited cup antenna and the DTU-ESA Spherical Near-Field Antenna Test Facility, Denmark, for measuring the breadboard. The work of Chalmers was partially funded by the Swedish Research Council and National Space Board grant (202-15).

References

[1] C. Cappellin et al., “Novel Multi-Beam Radiometers for Accurate Ocean Surveillance”, in Proc. EuCAP Conference, Den Haag, The Netherlands, 2014.

[2] P. W. Gaiser, et al., ”The WindSat Spaceborne Polarimetric Microwave Radiometer: Sensor Description and Early Orbit Performance”, IEEE Trans. Geo. Rem. Sensing, Vol. 42, No. 11, November 2004.

[3] http://nsidc.org/data/docs/daac/amsre_instrument.gd.html

[4] O. Iupikov et al., “Multi-Beam Focal Plane Arrays with Digital Beamforming for High Precision Space-Borne Ocean Remote Sensing”, IEEE Transactions on Antennas and Propagation, 2018, in press.

[5] C. Cappellin et al., “Design of a Push-Broom Multi Beam Radiometer for Future Ocean Observations” in Proc. EuCAP Conference, Lisbon, Portugal, 2015.

[6] J. Johansson and P. Ingvarson, “Array antenna activities at RUAG space: An overview,” in Proc. EuCAP Conference, Gothenburg, Sweden, 2013.

[7] O. A. Iupikov, A. A. Roev, and M. V. Ivashina, “Prediction of farfield pattern characteristics of phased array fed reflector antennas by modeling only a small part of the array – Case study of spaceborne radiometer antennas,” in Proc. EuCAP Conference, Paris, France, 2017.

[8] G. W. Kant, P. D. Patel, S. J. Wijnholds, M. Ruiter, and E. van der Wal, “EMBRACE: A multi-beam 20,000-element radio astronomical phased array antenna demonstrator,” IEEE Trans. Antennas Propag., vol. 59, no. 6, pp. 1990–2003, Jun. 2011.

[9] DTU-ESA Spherical Near-Field Antenan Test Facility, http://www.ems.elektro.dtu.dk/research/dtu_esa_facility

[10] J. R. de Lasson, C. Cappellin, K. Pontoppidan, O. Iupikov, M. Ivashina, N. Skou, and B. Fiorelli, “Innovative Multi-Feed-Per-Beam Reflector Antenna for Space-Borne Conical-Scan Radiometers”, submitted for AP-S/URSI (2018).